iJRASET
International Journal For Research in
Applied Science and Engineering Technology

INTERNATIONAL JOURNAL FOR RESEARCH

IN APPLIED SCIENCE & ENGINEERING TECHNOLOGY

Volume: 8 **Issue:** VII **Month of publication:** July 2020

DOI: https://doi.org/10.22214/ijraset.2020.30480

International Journal for Research in Applied Science & Engineering Technology (IJRASET)
ISSN: 2321-9653; IC Value: 45.98; SJ Impact Factor: 7.429
Volume 8 Issue VII July 2020- Available at www.ijraset.com

Formulation of a Catenoid Structured Wormhole without any Exotic Matter

Deep Bhattacharjee[1], Aruna Harikant[2], Sanjeevan Singha Roy[3]
[1]B.Com (Hons.), Calcutta University, West Bengal, Kolkata, India,
[2]Department of Physics, Sharda University, Greater Noida, U. P. – 201306, India
[3]Department of Physics, Birla Institute of Technology, Mesra, Ranchi, Jharkhand-835215, India

Abstract: Einstein-Rosen Bridge [1] introduced by Albert Einstein and Nathan Rosen, which arises as a solutions to Einstein-Field equations is not a new terminology. Extensive theoretical analysis has been made from different viewpoints but still, none of them has yet been discovered in reality. However, there lies a mild 'crack' to every solutions theorized, i.e. exotic energy is required for any wormhole constructions as this particular type of matter (or energy) would prevent the mouths of the wormhole from collapsing. No such constructive solutions has yet been discovered where there is no need of any exotic elements. These exotic elements are either possible in universe or not is still an open debate? Apart from that, the traversable nature of the wormholes is not at all possible except a few cases where also, there is need of exotic matters. Therefore, for general it can be said that the 'tunnels of time' or 'bridges connecting far space-times' either in our universe or from our universe to other universe is still unproven. Moreover, in addition to these, generally a wormhole is formulated as a Black Hole (BH) without any event horizon. The central singularity creates a problem, however if the singularity is 'Kerr or Ring' type then, this can be managed somehow, but how can one approaches towards singularity or even passing through them without being smeared into atoms? Additionally, the field equations of the General Theory of Relativity (GTR) allows travelling only from 'past to future' but not vice versa. Therefore, there are many constraints regarding the mechanics of the wormhole. This paper is mostly focused to eliminate above all constraints and thereby providing a feasible theoretical explanation of the 'time tunnel' using a different set of mathematics.

Keywords: Modified General Relativity; Einstein-Rosen Bridge; Raychaudhuri Equation; Lorentzian Wormhole; Null Energy Condition (NEC); Geodesics; deficit angle.

I. INTRODUCTION

A catenary curve is taken as the main ingredient of this thesis. It is then rotated along the axis of revolution to make a catenoid. Analysis has been done on this catenoid generating wormholes from **VI** sections, the section **I** relies heavily on the Newtonian-dynamics to generate the properties of the curve, along with the motion of a test particle m and its trajectory inside the wormhole from the perspectives of the horizon geometry, the force, gravitation, special relativistic effects and the 4-velocity, the centripetal force of the test mass paving the way for determining the potential and kinetic energy conditions on different regions of the wormhole by dividing it into 6 sub-parts as H^+, $\ell_0 - f$, $\overline{\mho}$, $\ell_1 - f$, H^- and deriving the amount of gravity acting on that particle by either increase in potential and decrease in kinetic, or decrease in potential and increasing in kinetic, deducing from the classical point of view the observable scenarios and effects of conversion from angular velocity to linear velocity and vice versa thereby providing a gateway for the conservation of energy and momentum. Sections **II III** and **IV** dives into the relativistic effects from GTR and modified gravity by considering the Raychaudhuri Equation proving that a NP-Null real tetrad l^μ drives geodesically through the generalized conic (with a deficit angle) of the wormhole with the maximum number of turns possible to execute the angular revolution around the boundary $\partial(G)$ of the wormhole, all without violating the NEC, meaning stress-energy-momentum tensor $T_{\mu\nu}$ is positive definite along the trajectory of the Null-rays. The gradient of the gravity $\nabla f(\partial(G))$ has been discussed along with the connection coefficients and Christoffel symbols for providing the two possible scenarios of a wormhole in inertial frame of reference and an wormhole in a non-inertial frame of reference to conclude the null acceleration vectors along $\ell_0 - f$ and $\ell_1 - f$ which ultimately leads to a geodesically congruence of $\sum l^n$ and the vanishing of the geodesics along $\overline{\mho}$ phase. Section **V** includes practical simulations. Section **VI** dictates the maximal load of wormhole before getting collapsed.

ISSN: 2321-9653; IC Value: 45.98; SJ Impact Factor: 7.429
Volume 8 Issue VII July 2020- Available at www.ijraset.com

A. Interpretation

1) The construction of the wormhole begins by taking a catenary curve having the equations,

$$\rho = c\, Cosh\, \frac{z}{c} \tag{1}$$

Where, c is a real constant and $c \neq 0$.

The surface of revolution of a catenary curve ρ along the vertical axis gives a 3-D catenoid having the revolution parameter φ satisfying the equation [2],

$$\oint_{\varphi} \rho = \mathbb{C} \tag{2}$$

Where $\mathbb{C}$ is the catenoid.

The parametric equations satisfying 3 coordinates x, y, z is,

$$x = c\, Cosh\left(\frac{v}{c}\right) Cos\, u \tag{3}$$

$$y = c\, Cosh\left(\frac{v}{c}\right) Sin\, u \tag{4}$$

$$z = v \text{ [3,4]} \tag{5}$$

Where $u\, \epsilon\, [-\pi, \pi]$, $v\, \epsilon\, \mathbb{R}$, $c \neq 0$ constant.

Therefore, the line element is,

$$ds^2 = Cosh^2\left(\frac{v}{c}\right) dv^2 + Cosh^2\left(\frac{v}{c}\right) du^2 \text{ [3,4]} \tag{6}$$

The Gaussian curvature is,

$$K = -\frac{1}{c^2} Sech^4\left(\frac{v}{c}\right) \text{ [3,4]} \tag{7}$$

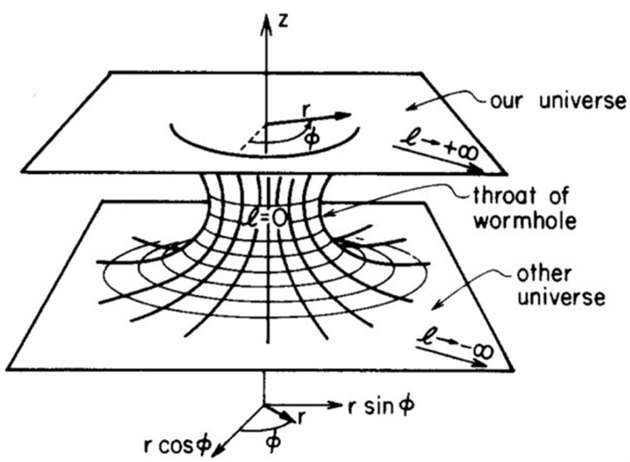

Fig.1 The wormhole with the catenoid structure, the catenary curve being the bold black lines. Figure from [5]

The worm hole has 2-Horizons, H^+ and H^- satisfying the equations,

$$Horizon = \begin{cases} H^+, \ Infalling\ (Source) \\ H^-, \ Outgoing\ (Destination) \end{cases} \tag{8}$$

The Cartesian coordinates having equal to both horizons as,

$$x = r\, Cos\, \Phi \tag{9}$$

$$y = r\, Sin\, \Phi \tag{10}$$

$$x, y = \begin{cases} x = r\, Cos\, \Phi, \ \ r\ (radius\ of\ H) \\ y = r\, Sin\, \Phi, \ \ \Phi = 360° \end{cases} \tag{11}$$

Our universe having a limit of distance $\ell_0 = +\infty$ and other universe having a limit of distance $\ell_1 = -\infty$. The traversable time for $\ell_0 = t_0$ and $\ell_1 = t_1$, $\ell_1 \gg \ell_0$ and $t_0 = t_1$ (time being constant through the wormhole although there lies a large spatial separation) such that the velocity *(V)* becomes,

$$V_{wormhole\ \mathbb{C}} = \frac{\int_{\ell_0}^{\ell_1} \ell\, d\ell}{\int_{t_0}^{t_1} t\, dt} \tag{12}$$

$\ell = 0$ is the middle of the throat of the wormhole which has the least curvature than ℓ_0 and ℓ_1. the region of maximum curvature $\mathcal{R}_{max}$ at $\ell_0 = \ell_1$ corresponds to a rotational velocity of the point mass m evolved through time $\dot{m}$ corresponds to a rotational velocity $V_{rot} = rm\dot{x}$ through a region of $\ell_0 - f$ and $\ell_1 - f$ such that,

$$\mathcal{R}_{max} \propto \ell_0 - f \tag{13}$$

$$\mathcal{R}_{max} \propto \ell_1 - f \tag{14}$$

Where f is the limiting radius of $\mathcal{R}_{max}$.

The **K**inetic **E**nergy (KE) of the 'test particle' is given by,

$$T = \frac{1}{2}m(r(f)^2)\omega^2 = \frac{1}{2}m(r(f)^2)\dot{\Phi}^2 \tag{15}$$

The Potential energy of the same 'test particle' is given by,

$$V = mgh \tag{16}$$

Then, the effective Lagrangian would be,

$$\mathcal{L}(\Phi, \dot{\Phi}) = \mathrm{T} - \mathrm{V} = \frac{1}{2}m(r(f)^2)\dot{\Phi}^2 - mgh \tag{17}$$

The momentum 'canonical to Φ' coordinate axis of rotation is,

$$P_\Phi = \frac{\partial \mathcal{L}}{\partial \Phi} = m(r(f)^2)\Phi = \mathrm{I}\omega = \boldsymbol{L} \tag{18}$$

Where I is the moment of inertia and L is the angular momentum which gives the expression,

$$\boldsymbol{L} = \boldsymbol{r} \times \boldsymbol{P} \tag{19}$$

Now, when the test mass 'm' crosses $\mathcal{R}_{max}$ the angular momentum $\boldsymbol{L}$ vanishes as $\boldsymbol{r}$ goes to zero, and the force vector **F** is perpendicular to the horizon H^+ *or* H^- of the catenoid C.

$$\mathbf{F} \perp \{(H^+)_C \text{ and } (H^-)_C\} \tag{20}$$

Then,

$$\boldsymbol{P} = \int_{t_0}^{t_1} \mathbf{F} \tag{21}$$

Here, $\boldsymbol{P}$ does not contain any Φ factor as the $\ddot{x}$ is linear and constant.

Now, the Energy-Momentum relation can be given by,

$$E = \sqrt{c^2p^2 + m^2c^4} + V \text{ [6]} \tag{22}$$

If the 3-velocity $\boldsymbol{u}$ can be stated as,

$$\boldsymbol{u} = u_x, u_y, u_z \text{ [7]} \tag{23}$$

Then,

$$E = \gamma_u mc^2 \tag{24}$$

And,

$$\boldsymbol{P} = \gamma_u m\boldsymbol{u} \tag{25}$$

γ_u is the Lorentz 'gamma' factor in the u frame given by,

$$\gamma_u = \sqrt{1 + \left(\frac{P_u}{mc^2}\right)} \tag{26}$$

Then,

$$E = mc^2\sqrt{1 + \left(\frac{P_u}{mc^2}\right)} \tag{27}$$

Equation (27) contains the potential energy while equation (18) is devoid of any potential energy. This can be assumed that, from the laws of conservation of energy,

$$T + V = 0 \tag{28}$$

Therefore, 3 conditions can be sufficed:

a) During $\ell_0 - f$ (infalling) phase, the rotational motion is so high that the KE dominates without **P**otential **E**nergy (PE) as seen from equation (1).

b) During the Throat-Falling Phase ($\overline{\mho}$) that is $\ell_0 - f < \overline{\mho} < \ell_1 - f$ the PE dominates and it is this excessive PE which makes the throat of the wormhole from collapsing, hence the wormhole is stable and traversable.

c) During the $\ell_1 - f$ (outgoing) phase the rotational motion is so high that the KE dominates without **P**otential **E**nergy (PE) as seen from equation (1).

The 3 sets of equations would be,

- $\ell_0 - f \rightarrow T(\uparrow) + V(\downarrow) = 0$
- $\overline{\mho} \rightarrow T(\downarrow) + V(\uparrow) = 0$
- $\ell_1 - f \rightarrow T(\uparrow) + V(\downarrow) = 0$

Where ↑ assigned the increment while ↓ is the decrement with T being KE and V being PE.

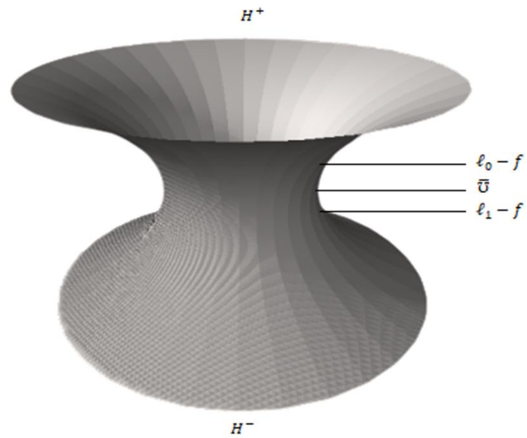

Fig. 2 Angular velocity takes place beyond $\ell_0 - f$ and $\ell_1 - f$ and linear velocity takes place at the region marked $\overline{\mho}$. The Horizons H^+ is at the top while H^- is at the bottom. (Picture Courtesy: Author: Polimerek; License: CC BY-SA 4.0, Source: Wikipedia Commons, Edit: Black background has been changed to white)

We can take an arbitrary frame of reference from horizon H^+, called it A. From this frame the test mass m can have a relation to the surrounding particles in the vicinity of H^+ and if this can be considered as the $Distance\ 0$ then, the other end of the horizon H^- can have the distance from the test particle m to H^- is $Distance\ \infty$. The gravitational relation (or the gravitational potential) between two cases $Distance\ 0$ and $Distance\ \infty$ can be represented taking $r = 0\ and\ \infty$ as,

$$Distance\ 0 \rightarrow -m \sum G \frac{m}{r} \rightarrow -m \sum G \frac{m}{0} = -\infty \tag{29}$$

This relation establishes that the horizon surface H^+ and H^- can have infinitely less gravitational potential.

$$Distance\ \infty \rightarrow -m \sum G \frac{m}{r} \rightarrow -m \sum G \frac{m}{\infty} = 0 \tag{30}$$

And then, as the particle moves towards the throat, the potential reduces to 0 from the reference frame of A.
However gravity exists in the zone $\overline{\mho}$ between $Distance\ 0 \ll \overline{\mho} \ll Distance\ \infty$ as,

$$-m \sum G \frac{m}{r} = K\ where\ K \neq 0 \tag{31}$$

The velocity is angular with an acceleration beyond $\ell_0 - f$ and $\ell_1 - f$ but is completely inertial and linear in the region between $\ell_0 - f$ and $\ell_1 - f$. This region is named here as $\overline{\mho}$. Here the 4-D velocity needs to be taken due to the relativistic nature of it, and can be defined as u^i as,

$$u^i = \frac{dx^i}{dt} = \left[\frac{dx^0}{dt}, \frac{dx^1}{dt}, \frac{dx^2}{dt}, \frac{dx^3}{dt}\right], [0\ being\ Time, 1,2,3\ being\ space\ dimensions] \tag{32}$$

The centripetal force of the angular orbit would have to make a transition phase from $\alpha(\complement) \rightarrow \beta(\complement)$ where $\alpha(\complement) = \ell_0 - f\ and\ \ell_1 - f$. Where as $\beta(\complement) = \overline{\mho}$.
$\alpha(\complement)$ is supported by an angular velocity and therefore a centripetal force (relativistic) acts on the test mass m given by,

$$F(\complement)_c = \sqrt{1 + \left(\frac{P_u}{mc^2}\right)}\left(\frac{2\pi}{T}\right) mv \tag{33}$$

Where T is the orbital period and when we take a limit as,

$$\lim_{T \rightarrow 0} \sqrt{1 + \left(\frac{P_u}{mc^2}\right)}\left(\frac{2\pi}{T}\right) mv = \infty \tag{34}$$

Therefore, the $F(\complement)_c$ for $\beta(\complement) = \overline{\mho} = 0$. This clearly indicates that angular velocity of $\alpha(\complement)$ region is converted to linear velocity then the centripetal force becomes infinite which thrashes out to behave like a linear velocity when the test particle m passes through $\beta(\complement)$.

2) Therefore, the traversal wormhole metric can be represented as,

$$ds^2 = -e^{2\varphi(u,v)}dt^2 + \frac{du^2 dv^2}{1-\frac{b(u,v)}{u,v}} + Cosh^2\left(\left(\frac{v}{c}\right)dv^2 + \left(\frac{v}{c}\right)du^2\right) \tag{35}$$

There is a finite function for the red-shift $\varphi(u,v)$ at H^+ to assume the absence of the event horizons. If the throat of the wormhole $b(u,v)$ has a clear geometry of flaring out conditions then the singularity won't exist as because,

$$1 - \frac{b(u,v)}{u,v} = 0 \tag{36}$$

Implies,

$$b(u,v) = 1 \tag{37}$$

The **N**ull **E**nergy **C**onditions (NEC) can be referred to the Raychaudhuri Equation as,

$$\frac{d\theta}{dr} = -\frac{1}{2}\theta^2 - \varepsilon_{\mu\nu}\varepsilon^{\mu\nu} + \xi_{\mu\nu}\xi^{\mu\nu} - R_{\mu\nu}l^\mu l^\nu \tag{38}$$

Where $R_{\mu\nu}$ is the Ricci-Tensor, l^μ be the NP-Null Tetrad, $\theta, \varepsilon_{\mu\nu}, \xi_{\mu\nu}$ being the expansion, shear and rotation respectively. The Null vector field l^μ refers to the test particle m as considered the equation (38) with the pure geometry of the space described by the equation (38) with no reference to any gravitational field. If the shear has a spatial signature $(-,+,+,+)$ with a unitary matrix 4*4 then the trace would become $Tr(-1,+1,+1,+1) = +2$ keeping the shear $\varepsilon^2 \equiv \varepsilon_{\mu\nu}\varepsilon^{\mu\nu} \geq 0$, the rotation parameter being $\xi^2 \equiv \xi_{\mu\nu}\xi^{\mu\nu} = 0$, then $R_{\mu\nu}l^\mu l^\nu \geq 0$. Now, in GTR, the EFE can be contracted as being the Einstein-Tensor $G_{\mu\nu} \equiv R_{\mu\nu} - \frac{1}{2}Rg_{\mu\nu} = l^\mu l^\nu T_{\mu\nu}$. This indicates that the Stress-energy-momentum tensor $T_{\mu\nu}l^\mu l^\nu \geq 0$. Now, in the modified theories of the gravity, the Einstein Tensor of the modified gravitational field gives an effective stress-energy-momentum tensor $T_{\mu\nu}^{eff}$ if and only if the Ricci Tensor in Raychaudhuri Equation is positive definite as $R_{\mu\nu}l^\mu l^\nu \geq 0$, then only $T_{\mu\nu}^{eff} \equiv T_{\mu\nu}^{eff}l^\mu l^\nu \geq 0$. This satisfies the NEC, however, the generalized NEC could be violates if Null-Vector l^μ enters in H^+ and defocused in H^-. This defocusing bundle of $\sum l^\mu$ could make the stress-energy relation $T_{\mu\nu}^{eff} \ll 0$ thereby violating NEC. This can be said as the congruence of Null geodesic violating NEC. If l^μ is normalized by multiplying with its covariant counterparts l_u, then the result becomes $l^\mu l_u = -1$. If l^μ is normalized and Ricci tensor $R_{\mu\nu}$ is positive definite, then from equation (38), the θ term could be replaced by T term as $T_{\mu\nu}^{eff}l^\mu l^\nu \geq -\frac{1}{2}T$. Now, the gravitational potential can be defined by $g_i(\sigma^j)$ where $i = 1\ or\ 2$. Where g_2 covers the coupling of $T_{\mu\nu}$ with matter. Now, $T_{\mu\nu}^{eff}$ can be represented by the equation,

$$T_{\mu\nu}^{eff} \approx (1 + g_i(\sigma^j))T_{\mu\nu} - \bar{D}_{uv} \tag{39}$$

$\bar{D}_{uv}$ can be taken as zero if we need original Einstein-Gravity and stating $g_i(\sigma^j) = 0$, one can obtain $T_{\mu\nu}^{eff} = T_{\mu\nu}$. And if,

$$(1 + g_i(\sigma^j))T_{\mu\nu} \ll \bar{D}_{uv}l^\mu l^\nu \tag{40}$$

Then,

$T_{\mu\nu}l^\mu l^\nu < 0$ and we obtain the general relation that NEC is violated. Setting $g_i(\sigma^j) = 0$ is a generalized form of Equation (30) regarding $Distance\ \infty$ from the Horizon (in-falling) H^+ to H^-.

Now, if $T_{\mu\nu}^{eff} < -\frac{1}{2}T^{eff}$ then this can be written as $T_{uv}l^u l^v - \frac{1}{2}T$ and similarly, $\bar{D}_{uv}l^u l^v - \frac{1}{2}\bar{D}$ and the bound between them can be explained by the following equations,

$$(1 + g_i(\sigma^j))\left[T_{\mu\nu}l^u l^v - \frac{1}{2}T^{eff}\right] \geq \left[\bar{D}_{uv}l^u l^v - \frac{1}{2}\bar{D}\right] \tag{41}$$

Then, as we have previously assumed $g_i(\sigma^j) = 0$ and $\bar{D}_{uv} = 0$, in the context of general relativity, then if $-\frac{1}{2}T^{eff} \approx -\frac{1}{2}T$, we can assume that $T_{\mu\nu}l^u l^v \geq \frac{1}{2}T$ which implies $T_{\mu\nu}l^u l^v \geq 0$ and NEC is satisfied. If the stress-energy-density is measured as positive definite by $T_{\mu\nu} \geq 0$ then, this entails the $T_{\mu\nu} = diag[-\rho(\mu,\nu), p(\mu,\nu), p(\mu,\nu), p(\mu,\nu)]$ by moving the NP-Null geodesic l^u via the 4-velocity vector u^i as in equation (32). [8]

3) The wormhole in Fig. 2 describes the wormhole as a set of 2 cones with a deficit angle. The first cone is in upright from the bottom having a deficit angle connected with another cone downwards with another deficit angle. The region bounded by the deficit angle is the minima point (without any singularity) as the throat factor $b(u,v)$ in equation (35) and (36) describes the region previously mentioned as $\overline{\mho}$. Here the linear motion dominates because the geodesic trajectory is being vanished at this region. Therefore, the NP-Null vector l^u which has the velocity components (being a vector as magnitude and direction), the magnitude remaining the same, however, the direction alters and therefore, can be expressed as a 4-acceleration vector of two types,

The inertial frame of the wormhole coordinates are static in hyperspace given by A as,

$$\frac{dU}{d\tau} = \left(\gamma_u^4 \frac{a \cdot u}{c}, \gamma_u^4 \left(a + \frac{u \times (u \times a)}{c^2}\right)\right) \text{ [9,10]} \tag{42}$$

Where U is the 3-velocity, a is the 3 acceleration and γ_u is the Lorentz-gamma factor.

The non-inertial frame if the wormhole mouths are not static in hyperspace, this can be one wormhole mouth, moving relative to the other thereby the coordinates could be accelerated given by A^ψ as,

$$\frac{DU^\psi}{d\tau} = \frac{dU^\psi}{d\tau} + \Gamma^\psi{}_{\mu\nu} U^\mu U^\nu \tag{43}$$

Where $\Gamma^\psi{}_{\mu\nu} = 0$ if inertial coordinates and $\Gamma^\psi{}_{\mu\nu} \neq 0$ if non-inertial coordinates.

However, beyond the phase $\ell_0 - f$ and $\ell_1 - f$ there exists geodesic motion with no acceleration of l^u,

$$\nabla_{\dot{\gamma}} \dot{\gamma} = 0 \tag{44}$$

Where ∇ is the covariant derivative and $\dot{\gamma}$ is the derivative with respect to time.

Equation (44) can be expanded as,

$$\frac{d^2\gamma^\psi}{dt^2} + \Gamma^\psi{}_{\mu\nu} \frac{d\gamma^\mu}{dt} \frac{d\gamma^\nu}{dt} = 0 \tag{45}$$

Where $\Gamma^\psi{}_{\mu\nu}$ is the Christoffel symbol or connection coefficient of the derivative operator ∇ with $\gamma^\mu = x^\mu \circ \gamma(t)$ and $\gamma^\nu = x^\nu \circ \gamma(t)$ of the $\gamma(t)$ curve.

4) The catenoid has a surface gravity as $\partial(G)$ which makes the Null-rays l^u followed a geodesic path as described by the surface integral (the 2D surface inside the cone) given by,

$$\iint_{\partial(G)} l^u = \Delta_0 \tag{46}$$

The gradient of the gravity of a 3-D catenoid is defined by definition,

$$\nabla f(\partial(G)) = \begin{bmatrix} \frac{\partial f}{\partial x} \partial(G) \\ \frac{\partial f}{\partial y} \partial(G) \\ \frac{\partial f}{\partial z} \partial(G) \end{bmatrix} \neq 0 \tag{47}$$

Now, if l^u is at the boundary region at the base of the conic circumference $2\pi R$, R being the radius of horizon H^+, it will try to move upward towards $\overline{\mho}$ by crossing $\ell_0 - f$ and then entering $\ell_1 - f$ after passing through $\overline{\mho}$. Therefore, in the regions beyond $\overline{\mho}$ it will try to follow the minimum path from H^+ to $\overline{\mho}$ thereby attaining a geodesic. The geodesic would be there beyond $\ell_0 - f$ and $\ell_1 - f$ but deduced to a straight line in $\overline{\mho}$.

Preserving the Z-coordinate, the projection onto XY-plane can be described by the coordinates ρ and φ given,

$$x = \rho \, Cos \, \varphi \tag{48}$$

$$y = \rho \, Sin \, \varphi \tag{49}$$

The starting point of l^u on the 2-D boundary $\partial(G)$ is best described by,

$$\rho = \rho_0 \tag{50}$$

$$\varphi = -\varphi_0 \tag{51}$$

Therefore, the coordinates at the end point would be given by,

$$\rho = \rho_0 \tag{52}$$

$$\varphi = \varphi_0 + 2\pi n \, , n \in \mathbb{N}_0 \tag{53}$$

As the axially symmetric nature of the cone is always on Z-axis, then when the journey of l^u on the 2-D boundary $\partial(G)$ begins at the cone base, the total angle subtended by the endpoints is $2\varphi_0$. However, the end points has been defined as an angular coordinate

$\varphi_0 + 2\pi n$ with n as a non-negative integer and $2\pi n$ is used to circumvent the cone before reaching the end point of the deficit angle, that is the region marked as $\overline{\mho}$ in Fig. 2. Therefore, the path of l^u parameterized by the geodesic is,

$$\rho(\varphi) = \rho_0 \left(\frac{Cos(Sin\,\theta(\varphi_0+n\pi))}{Cos(Sin\,\theta(\varphi-n\pi))}\right) \quad (54)$$

This equation describes the variation of angle with the distance along Z-coordinates from the base. Three conditions for θ needs to be satisfied as,

a) $\theta = 0°$ (the geodesic is a circle)
b) $\theta = 90°$ (the geodesic is a straight line)
c) $\theta = 180°$ (the geodesic absorbs in the circumference and then moves out of the circumferential surface)

As l^u gets closer and closer to $\overline{\mho}$, the geodesics start to flatten and at $\overline{\mho}$, the geodesics simply vanish giving away 2 straight lines, one from the start point to the deficit angular end, the other from the angular end to the end point. The denominator of the equation (54) cannot be zero or negative as this simply destroys the geodesic equation. Therefore, the sensible values can only happen when,

$$Sin\,\theta(\varphi_0 + n\pi) < \frac{\pi}{2} \quad (55)$$

$$Sin\,\theta(\varphi - n\pi) < \frac{\pi}{2} \quad (56)$$

$$\theta_n = arcsin\left(\frac{1}{2n}\right) \quad (57)$$

Where n denotes the number of turns of l^u along $\partial(G)$ to reach $\overline{\mho}$ [11].

5) Simulations have been provided with 2 parameters [12],

- $y = a\,Cosh\left(\frac{x}{a}\right) + C$
- $y = ax^2 + bx + c$

BLACK → b and RED → a, C

b for equation $ax^2 + bx + c$ and a, C for equation $a\,Cosh\left(\frac{x}{a}\right) + C$

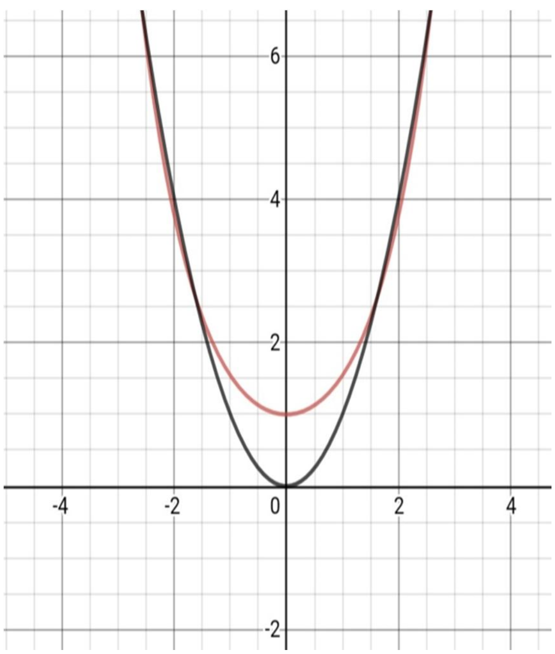

Fig. 3 b = 0, a = 1, C = 0 showing a parabolic catenary

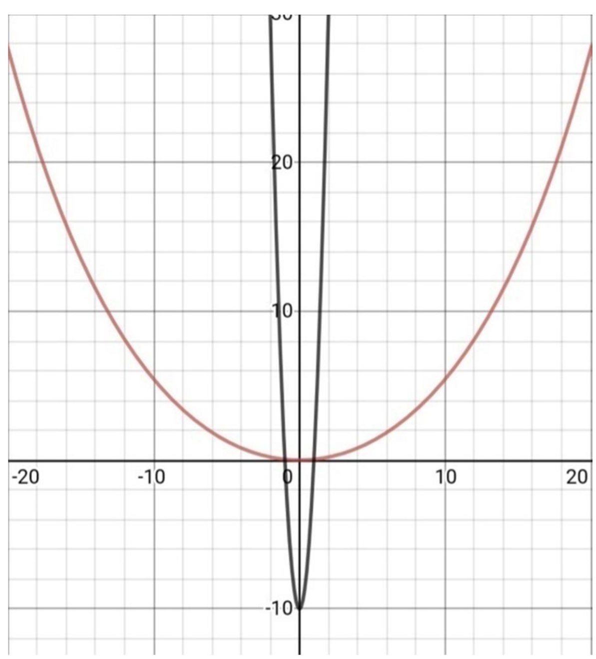

Fig. 4 b = 0, a = -10, C = -10 showing a wide catenary

ISSN: 2321-9653; IC Value: 45.98; SJ Impact Factor: 7.429
Volume 8 Issue VII July 2020- Available at www.ijraset.com

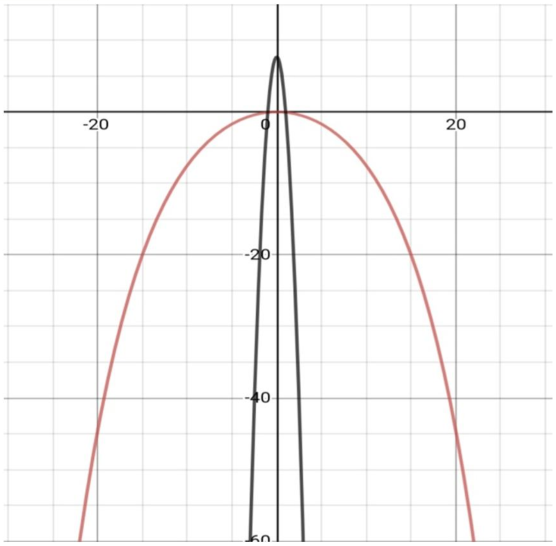

Fig. 5 b = 0, a = -7.7, C = 7.7 showing a parabolic inverted catenary

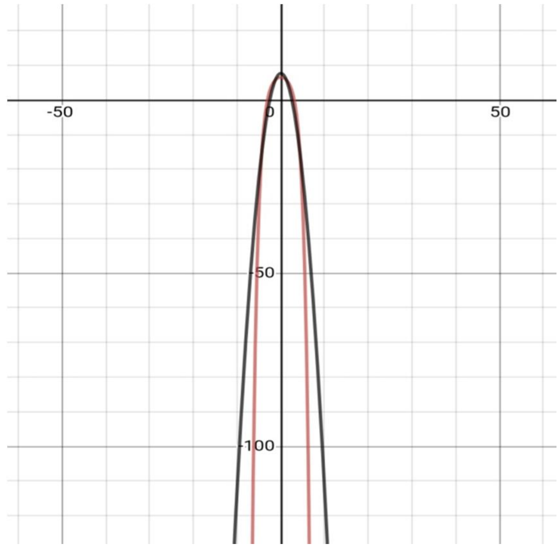

Fig. 6 b = 0, a = -1.2, C = 7.7 showing a parabolic narrow inverted catenary

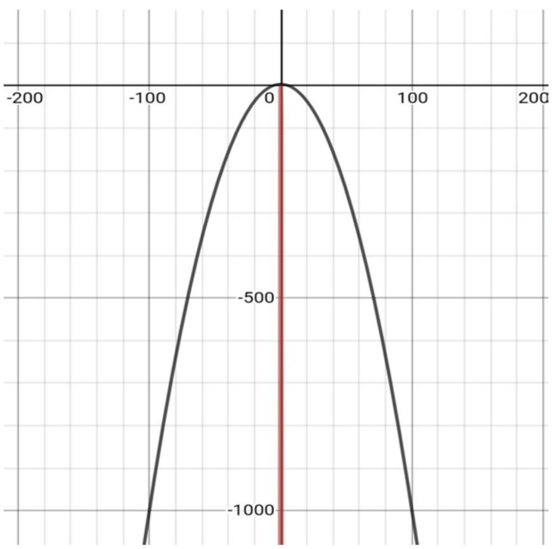

Fig. 7 b = 0, a = -0.1, C = 3.2 showing a collapsed Catenary

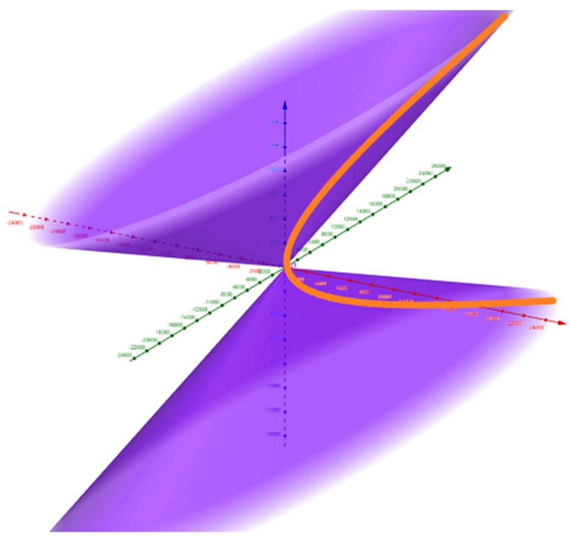

Fig. 8 Summing up the catenoid with the catenary curve in a 3-dimensional plane (X,Y,Z).

6) Generally, a wormhole has 2 mouths. In some special cases the mouths can vary upto 3 and 4. However, considering the wormhole having 2 mouths, one mouth is separated by the other mouth via a large distance and the mouths are floating in hyperspace. One mouth is always in relative motion of the other mouths, this generally happens due to the large spatial and temporal limits between two mouths moving relative to each other. If a Null-vector l^u enters the throat of the wormhole as depicted by $\overline{\mho}$, then the geodesic motion vanishes and linear motion dominates along the inner boundary region $\overline{\mho}_{\partial(G)}$ where the Null-vector l^u gets trapped and due to the relativistic effects of the movement of wormhole mouths, the light rays (or $\sum l^u$) passes erratically through the throat $\overline{\mho}$ which superimposed by the relativistic motions gets Doppler-Boosted and therefore gets more blue shifted with a high frequency, high energy and small wavelength as,

$$f_r = \frac{1}{\sqrt{1-\left(\frac{v}{c}\right)^2}} f_s \qquad (58)$$

This Doppler-Boost would have increased the flux density of $\sum l^u$ along the surface $\overline{\mho}_{\partial(G)}$ which points that the light ray moves back and forth from one mouth to another getting boosted, again moves from the other mouth to origin, again getting boosted which

International Journal for Research in Applied Science & Engineering Technology (IJRASET)
ISSN: 2321-9653; IC Value: 45.98; SJ Impact Factor: 7.429
Volume 8 Issue VII July 2020- Available at www.ijraset.com

results in the pile up of radiation on the throat $\overline{\mho}_{\partial(G)}$. This radiation pile up occurs as the density of the flux ϕ_S increases and tends towards infinity. The flux density can be given by means of the surface integral,

$$\phi_S = \oiint_{Area} \overline{\mho}_{\partial(G)}\, d\boldsymbol{A} \tag{59}$$

With the condition,

$$\lim_{\phi_S \to \infty} \phi_S = \oiint_{Area} \overline{\mho}_{\partial(G)}\, d\boldsymbol{A} \tag{60}$$

This creates a huge radiation pressure on the wormhole throat $\overline{\mho}$ given by,

$$P_{Rad} = \frac{\langle S \rangle}{c} \tag{61}$$

Where, S is the magnitude of the Poynting-vector and c is the speed of the light.

However, if the motion of the 2 mouths of the wormhole starts to moving at speeds close to that of light and if it happens for a particular amount of time then c gets dilated and almost stops going to 0, thereby happening a dangerous condition as,

$$P_{Rad} = \frac{\langle S \rangle}{c} = \frac{\langle S \rangle}{0} = \infty \tag{62}$$

The radiation pressure P_{Rad} goes to infinity and the wormhole degenerates from the throat making the 2 mouths separable without any bridges or affine connections between them.

Before the throat collapses the mapping f_U can be done along each and every phases of the catenoid by,

$$f_U \to H^+ \cap \ell_0 - f \cap \overline{\mho} \cap \ell_1 - f \cap H^- \tag{63}$$

However, after the throat collapses the mapping f_U splits into 2 parts given,

$$\overline{\mho}\ disappears = \begin{cases} 1_{f_U} \to H^+ \cap \ell_0 - f \\ 2_{f_U} \to \ell_1 - f \cap H^- \end{cases} \tag{64}$$

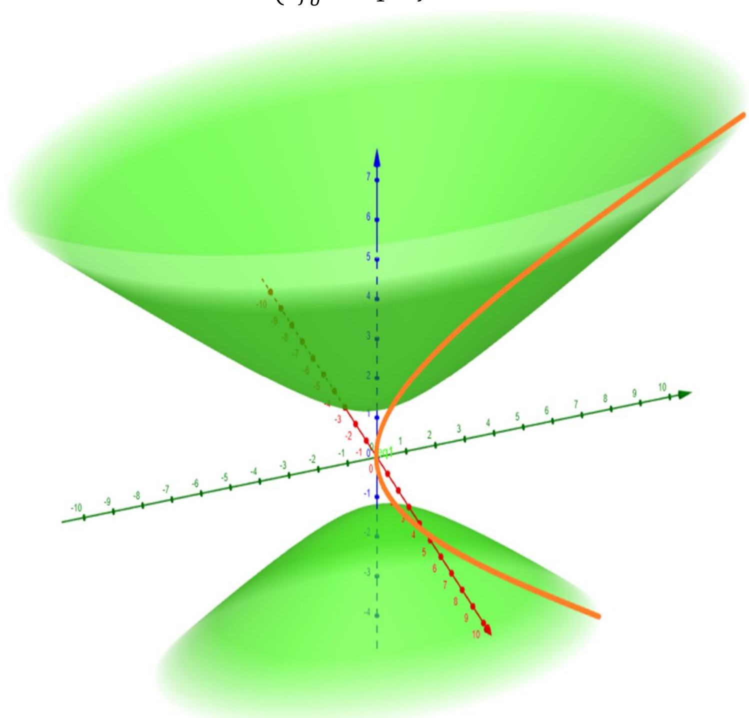

Fig. 9 The collapsing of the wormhole throat $\overline{\mho}$ results the wormhole splits into 2 parts 1_{f_U} and 2_{f_U} from f_U.

This is best described by the equation of Hyperboloid of 2 sheets as,

$$-\frac{x^2}{a^2} - \frac{y^2}{b^2} + \frac{z^2}{c^2} = 1 \tag{65}$$

Moreover the Hyperboloid of 2 sheets cannot have any catenary curve (as seen disjoint from **Fig. 9**).

International Journal for Research in Applied Science & Engineering Technology (IJRASET)
ISSN: 2321-9653; IC Value: 45.98; SJ Impact Factor: 7.429
Volume 8 Issue VII July 2020- Available at www.ijraset.com

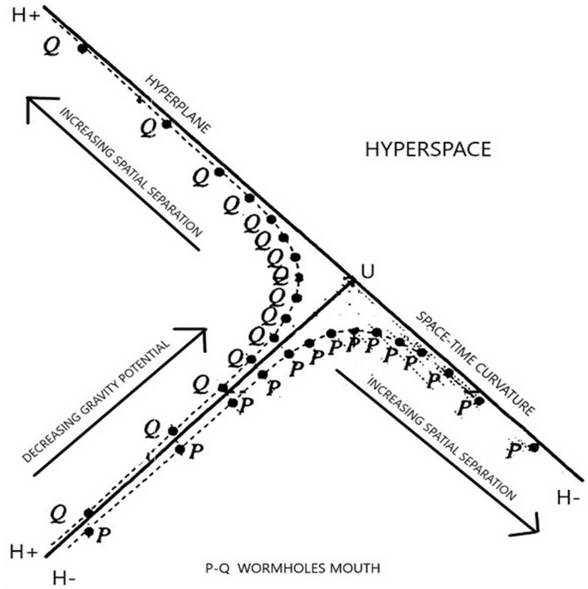

Fig. 10 In this diagram Q represents $\ell_0 - f$ with horizons H^+ while P represents $\ell_1 - f$ with horizons H^- , the separating line U represents the wormhole throat $\overline{\mho}$ with P and Q getting further from each other as 'gravity potential decreases' and 'spatial separation increases marked with a boundary of 'hyperplane', all existing in 'hyperspace'. Picture Courtesty: (Throne, K. S., 1993. Closed Timelike Curves. *Theoretical Astrophysics. California Institute of Technology Pasadena* pp. 7 Fig. 4), the figure has been modified for the purpose of this paper.

II. CONCLUDING REMARKS

The paper discussed wormhole generation and its basic properties from both Newtonian mass and relativistic null vectors, all without violating the NEC. Extensive analysis has been done from all the possible aspects and modified field equations of GTR has been accessed to prove the stress-energy-momentum tensor positive definite, all with the background of the laws of conservation of energy and the maximal radian pressure that the wormhole can handle before getting collapsed. 2D and 3D plotting have been provided for a better visualization of the parametric curve and equations.

REFERENCES

[1] Einstein, A. and Rosen, N., 1935. The Particle Problem in the General Theory of Relativity. Physical Review, 48(1), pp.73-77.
[2] Dierkes, U., Hildebrandt, S., Sauvigny, F. and Tromba, A., 2010. Minimal Surfaces. Heidelberg: Springer.
[3] Archive.lib.msu.edu. 2020. Catenoid. [online] Available at: <https://archive.lib.msu.edu/crcmath/math/math/c/c111.htm> [Accessed 8 July 2020].
[4] Fischer, G., 1986. Mathematical Models From The Collections Of Universities And Museums. Braunschweig: F. Vieweg & Sohn, p.43
[5] Morris, M. and Thorne, K., 1988. Wormholes in spacetime and their use for interstellar travel: A tool for teaching general relativity. American Journal of Physics, 56(5), pp.395-412.
[6] Eisberg, R., Resnick, R. and Derringh, E., 1985. Quantum Physics Of Atoms, Molecules, Solids, Nuclei And Particles. New York: John Wiley.
[7] Kleppner, D., Kolenkow, R. and Kolenkow, R., n.d. An Introduction To Mechanics.
[8] Harko, T., Lobo, F., Mak, M. and Sushkov, S., 2013. Modified-gravity wormholes without exotic matter. Physical Review D, 87(6).
[9] Pauli, W., 1981. Theory Of Relativity. New York: Dover Publications, p.74.
[10] Synge, J. and Schild, A., 1962. Tensor Calculus, By J.L. Synge And A. Schild. Toronto: University of Toronto Press, pp.149, 153, 170.
[11] Conversation of Momentum. 2020. Geodesics On A Cone. [online] Available at: <https://conversationofmomentum.wordpress.com/2014/09/07/geodesics-on-a-cone/> [Accessed 8 July 2020].
[12] Desmos. 2020. Catenary. [online] Available at: <https://www.desmos.com/calculator/1lfpgnpoko> [Accessed 9 July 2020].

End Notes:

Fig. 8 and **Fig. 9** are plotted in https://www.geogebra.org/3d?lang=en
Figures have been drawn and modified using MS-Paint 3D.
References have been generated using: https://www.citethisforme.com/citation-generator/apa
Authors of this paper have no competing interests.
© Authors

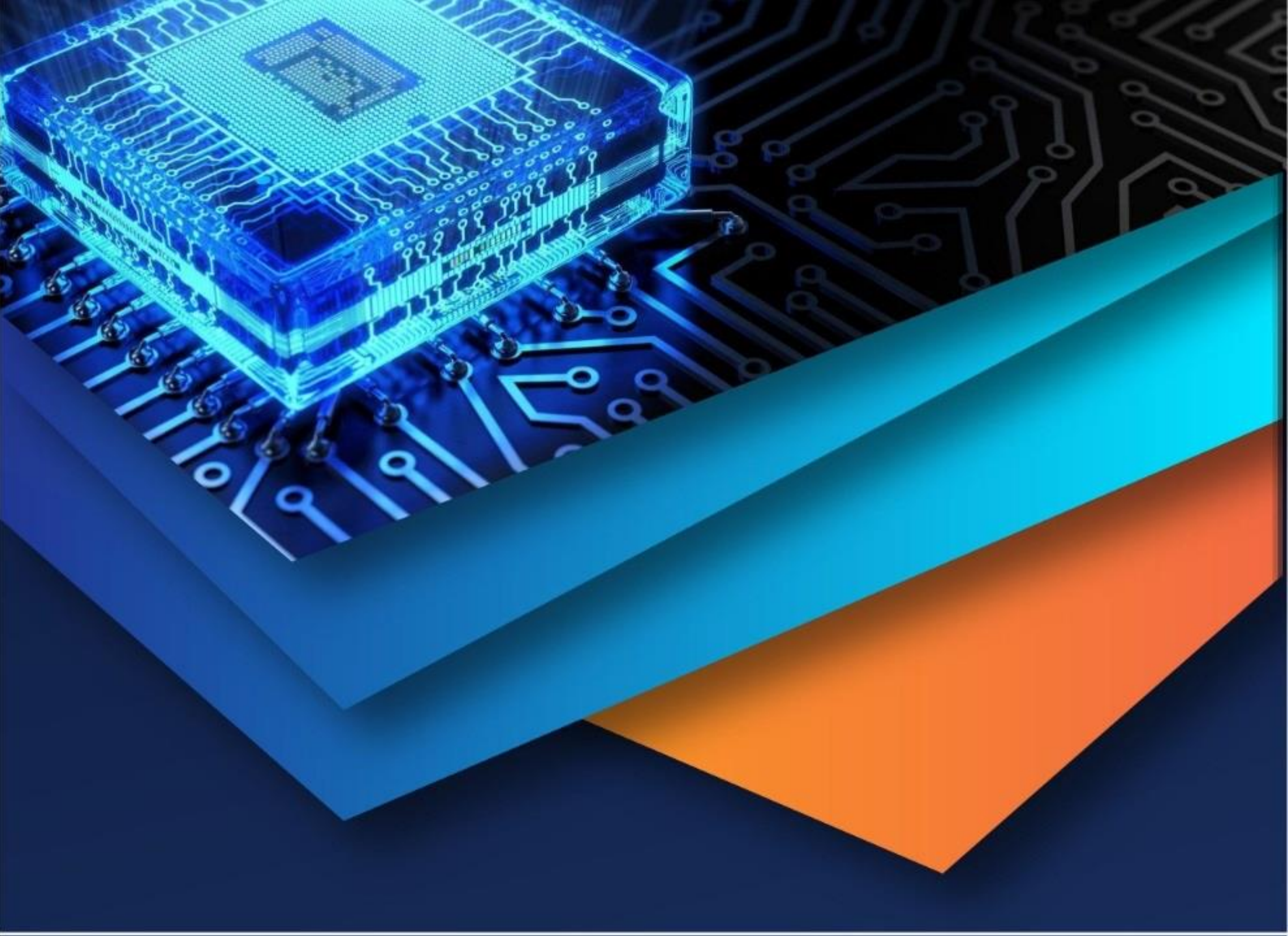

10.22214/IJRASET

45.98

IMPACT FACTOR: 7.129

IMPACT FACTOR: 7.429

INTERNATIONAL JOURNAL FOR RESEARCH

IN APPLIED SCIENCE & ENGINEERING TECHNOLOGY